Int. J. Multiphase Flow Vol. 19, No. 1, pp. 91–97, 1993
Printed in Great Britain.

0301-9322/93 $6.00 + 0.00

EFFECT OF HELICAL WIRES ON THE LIQUID FILM STRUCTURE IN A TWO-PHASE ANNULAR MIST FLOW

S. NAMIE and K. SHIOZAKI
Power and Energy Engineering Division, Ship Research Institute, Shinkawa, Mitaka, Tokyo 181, Japan

(Received 13 June 1991; in revised form 30 August 1992)

Abstract—Previously, it has been reported that the total amount of entrained droplets in a two-phase annular mist flow in tubes with helical-wired or ribbed inner surfaces decreases as compared with that in a smooth tube, and an empirical correlation for the entrainment suppression proposed. Furthermore, it has been suggested that the decrease in the number and deformation of disturbance waves on the liquid film surface may be the cause of the entrainment suppression. The aim of the present paper is to investigate which of two effects is the main cause of the wave deformation: the smoothing effect on the liquid film caused by the centrifugal force of the swirling motion; or the direct interaction between the waves and the helical obstacles. To this end, the interfacial and inner structures of the liquid film are investigated in a channel between coaxial double tubes where the centrifugal force acts in the inverse direction. From measurements of the liquid film via an electrical conductance method, it is shown again that the disturbance waves on the liquid film surface are reduced in number and changed from the original shape by the helical wires on the column as compared with those on the smooth surface. It results that the mean thickness of the liquid film and the number of waves on the film increase greatly just upstream of the wires. Furthermore, a secondary flow can be observed in the bottom layer of the film flow by visualization with an "oil film" method. These results suggest that the helical obstacles break the disturbance waves into comparatively small waves. On the other hand, the smoothing effect caused by the centrifugal force of the swirling motion is estimated to be small. Therefore, the direct interaction between the waves and the helical obstacles described above seems to be the main cause of the deformation of the disturbance waves.

Key Words: gas–liquid multiphase flow, annular mist flow, helical wires, liquid film structure, droplet-entrainment suppression, number of disturbance waves, secondary flow

1. INTRODUCTION

In the high steam-quality range of two-phase fluids in steam generators of the once-through type (e.g. a boiler, a nuclear reactor steam generator, heat pump evaporators etc.), a large amount of liquid droplets are entrained into the core region of the evaporation tubes. This causes liquid film dryout on the tube wall and a reduction in the evaporative heat transfer rate, it also prevents the gas phase from becoming dry downstream of the tubes.

In a former study (Namie & Shiozaki 1991), with the aim of improving the evaporative heat transfer by reducing the amount of droplets, the authors investigated experimentally the characteristics of a two-phase annular mist flow in tubes with helical-wired or ribbed inner surfaces for various helical sizes and gas/liquid flow rates. It was reported that the total amount of entrained droplets in the annular mist flow in the tubes decreases as compared with that in a smooth tube, and the following empirical correlation was proposed for the entrainment suppression:

$$E/E_s = \mathrm{k}\ n^{\mathrm{i}} \times (\pi\ D/p)^{-0.353}/(d/\delta), \qquad [1]$$

where E denotes the mass flow ratio of the entrained droplets to the total liquid flow rate, and the subscript s represents the value of E in the smooth tube; n, p and d are the number, pitch and height of the helical wires, respectively, k and i are empirical constants, D is the inner tube diameter and δ is the maximum thickness of the liquid film, i.e. the distance from the tube surface to the wave crest, obtained in the smooth tube.

Figure 1 [also presented in Namie & Shiozaki (1991)] shows the correlated data with [1] for all the test tubes with helical obstacles shown in figure 2 and summarized in table 1. Furthermore, the authors have suggested that the disturbance waves on the liquid film surface decrease in number and change from the original shape as compared with those in the smooth tube, shown in figure 3, which should be one of the causes of the entrainment suppression (Namie & Shiozaki 1990, 1991; Shiozaki & Namie 1991).

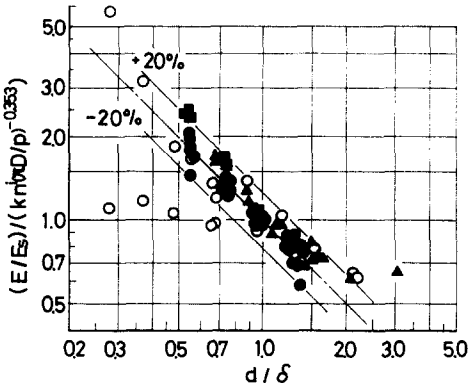

Figure 1. Entrainment correlated with [1].

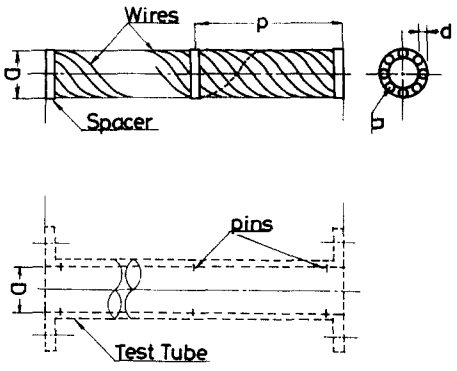

Figure 2. Inner-wired type test tube.

The aim of the present paper is to investigate which of two effects is the main cause of the wave deformation: the smoothing effect on the liquid film caused by the centrifugal force of the swirling motion; or the direct interaction between the waves and the helical obstacles. To this end, the interfacial and inner structures of the liquid film are investigated together with the entrainment rate in a channel between coaxial double tubes with a helical-wired outer surface of the inner column.

Although there have been some reports on two-phase flow in rifled tubes (Iwabuchi *et al.* 1982; Köhler & Kastner 1986; Yoshida *et al.* 1988), the effect of spiral wires on liquid film structures has never been investigated in connection with the reduction of droplet entrainment.

2. EXPERIMENTAL APPARATUS AND MEASUREMENTS

2.1. Test channels and experimental conditions

Figure 4 is a schematic diagram of the test channel of double-tube type, in which a two-phase mixture of air and water flows at atmospheric pressure. The auxiliary equipment for the test is almost the same as that for the inner-wired tube which was investigated in former studies (Namie & Shiozaki 1990, 1991). The channel consists of coaxial double tubes, 3 m long, and is made of acrylic resin. Water is introduced into the channel through a cylindrical sinter section at the bottom of the inner column and then mixed with air in order to produce annular mist flow. The liquid film flowing on the surface of the inner column and the large amount of liquid droplets entrained

Table 1. Symbols and sizes of the test tubes in figures 1 and 2 and the liquid flow rate

Symbol	No. of tubes	Rib height × breadth (mm)	Wire dia, d (mm)	Wire helical pitch, p (mm)	No. of wires, n	Total liquid flow W_L (kg/s)	Total liquid flow U_L (m/s)	Parameter $\pi D/p$
	No. 1 Smooth	—	—	—	—	0.083	0.279	—
	No. 1 Smooth	—	—	—	—	0.050	0.167	—
	No. 1 Smooth	—	—	—	—	0.033	0.112	—
	No. 1 Smooth	—	—	—	—	0.017	0.056	—
	No. 2 Straight-ribbed	1.0 × 5.0	—	∞	8	0.083	0.279	0.0
○	No. 3 Helical-ribbed	1.0 × 5.0	—	1000	8	0.083	0.279	0.061
○	No. 4 Helical-ribbed	2.0 × 2.5	—	1000	8	0.083	0.279	0.061
○	No. 5 Helical-ribbed	—	3.2	500	4	0.083	0.279	0.122
●	No. 6 Helical-wired	—	2.0	200	16	0.083	0.279	0.306
●	No. 7 Helical-wired	—	2.0	200	8	0.083	0.279	0.306
▲	No. 7 Helical-wired	—	2.0	200	8	0.050	0.167	0.306
▲	No. 7 Helical-wired	—	2.0	200	8	0.033	0.112	0.306
▲	No. 7 Helical-wired	—	2.0	200	8	0.017	0.056	0.306
●	No. 8 Helical-wired	—	2.0	200	4	0.083	0.279	0.306
●	No. 9 Helical-wired	—	2.0	200	3	0.083	0.279	0.306
●	No. 10 Helical-wired	—	2.0	200	2	0.083	0.279	0.306
●	No. 11 Helical-wired	—	2.0	200	1	0.083	0.279	0.306
■	No. 12 Helical-wired	—	2.0	800	4	0.083	0.279	0.077
■	No. 13 Helical-wired	—	2.0	400	4	0.083	0.279	0.153
■	No. 14 Helical-wired	—	2.0	100	4	0.083	0.279	0.612
○	No. 15 Helical-wired	—	1.0	200	4	0.083	0.279	0.306

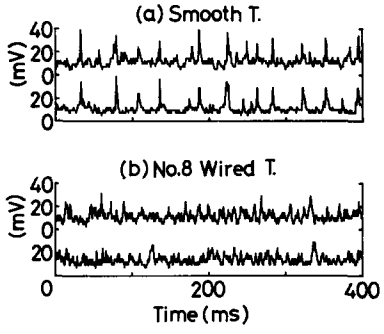

Figure 3. Fluctuation of the liquid film thickness in the (a) smooth tube and (b) inner-wired tube.

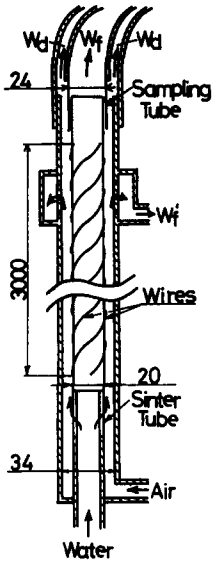

Figure 4. Double-tube type test channel.

in the gas core flow are divided mutually by a sampling tube positioned downstream of the test channel and separated from the gas phase flow by two cyclone separators.

A specific number of helical wires with a circular cross-section made of polyvinyl chloride resin are wound on the outer surface of the inner column. It should be emphasized that the centrifugal force of the swirling motion caused by the helical obstacles in the present test channels acts in the inverse direction as compared with that in the inner-wired tubes tested in the former studies shown in figure 2. Table 2 summarizes the sizes of the helical wire together with the symbols for figure 6 corresponding to each of the channels. The diameter D of the inner column is 20 mm, while the inner diameter of the outer tube is 34 mm. The height d, helical pitch p and number n of the wires are 2, 200 and 400 mm and 4, respectively. The total liquid flow rate W_L is also indicated in table 2.

In addition to these test channels, the "mono-wired" channel, which consists of the column on the outer surface of which only one helical wire of one pitch long is wound, is used in order to investigate the direct interaction between the disturbance waves and the helical obstacles.

2.2. Measurements of each flow rate and the liquid film structure

In figure 4, W_f denotes the liquid film flow rate on the surface of the inner column, W_f' is the liquid film flow rate on the inner surface of the outer tube and W_d represents the flow rate of droplets entrained in the gas-phase flow. Each value of the flow rates was obtained via the following procedure: Firstly, W_f and $W_f' + W_d$ were separated with a sampling tube of $D_s = 24$ mm i.d. and measured independently with a measuring cylinder and a stopwatch; after substituting the outer tube equipped with a porous section, as shown in figure 4, for one without a porous section, the liquid film flow rate W_f' extracted from the porous section was measured under the same two-phase flow conditions; from these measurements, W_f, W_d and W_f' were determined individually.

As described above, a sampling tube of fixed inner diameter was used in the present experiment just as in the former study (Namie & Shiozaki 1990), where the diameter was estimated from the

Table 2. Symbols and sizes of the test channels in figure 4 and the liquid flow rate

Symbol	No. of tubes	Wire dia, d (mm)	Helical pitch p (mm)	No. of wires, n	Total liquid flow W_L (kg/s)	Total liquid flow U_L (m/s)
▼	No. 1 Helical-wired	2.0	200	4	0.050	0.265
▽	No. 1 Helical-wired	2.0	200	4	0.033	0.176
■	No. 2 Helical-wired	2.0	400	4	0.050	0.265
□	No. 2 Helical-wired	2.0	400	4	0.033	0.176

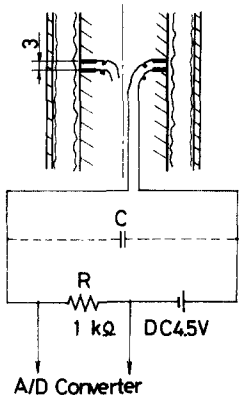

Figure 5. Liquid film measurement.

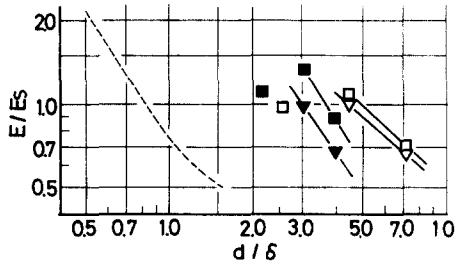

Figure 6. Entrainment in the double-tube type channel.

data of the maximum liquid film thickness and selected in such a way that a part of liquid film was never collected together with droplets for all of the flow conditions. The measurements, therefore, may slightly underestimate the total entrainment. The underestimation should not be too great, since the local flow rate of the droplets is usually very low near the liquid film surface.

The interfacial structure of the liquid film was measured with an electrical conductance method. Figure 5 shows the conductance probes used, which are almost the same as those employed previously. Two pairs of electrodes, for measuring the local conductance of the liquid film, were positioned facing each other on opposite sides of the column wall. The output voltage in the conductance method is nearly proportional to a local thickness of the liquid film.

On the other hand, the "oil film" method was used to visualize the inner structure of the liquid film flow adjacent to the column surface.

3. RESULTS ON THE ENTRAINMENT AND THE INTERFACIAL STRUCTURE

As shown in figure 3, the disturbance waves on the liquid film surface decrease in number and the film surface is smoothed by installation of the helical obstacles on the walls of the test tubes. It has been pointed out by former investigators that the droplets are produced mainly from the crests of the annular disturbance waves. Hence, the decrease in the number and deformation of the waves should be one of the causes of the entrainment suppression, as described previously (Namie & Shiozaki 1990, 1991; Shiozaki & Namie 1991).

Two explanations are considered for the decrease in the number and deformation of the waves; the first is the direct interaction between the waves and the helical obstacles; the second is the centrifugal force induced by the swirling motion of the fluid, since, in inner-wired tubes which were investigated in previous studies, the force acts towards the tube wall and may smooth the liquid film surface. Therefore, in order to investigate which one of the above two phenomena is dominant, the test in a double-tube type channel was performed, where the centrifugal force acts in the inverse direction.

Figure 6 shows the results of the entrainment in the channel expressed with the same nondimensional numbers, E/E_s and d/δ, as used in figure 1. The representative data in the former studies, corresponding to figure 1, are also indicated by the dotted line. In the figure, an increase in the value of d/δ means, for constant values of d and W_L, that the gas velocity, and hence the liquid film velocity, increase. The centrifugal force of the swirling motion, therefore, increases as the value of d/δ becomes large. It should be noted that E/E_s decreases with almost the same gradient as for the former data, irrespective of the difference in the direction of the centrifugal force.

Figure 7 shows a comparison between two output voltages measured by the electric conductance method at the same axial position of the column. In the smooth column, part (a), large peaks corresponding to the disturbance waves are obtained simultaneously on opposite sides of the column circumference. In the wired column, part (b), the large peaks measured at the middle of a span between two wires decrease in number and the liquid film surface becomes comparatively smooth. Further, the coincidence of peaks obtained at the two positions becomes unclear. These

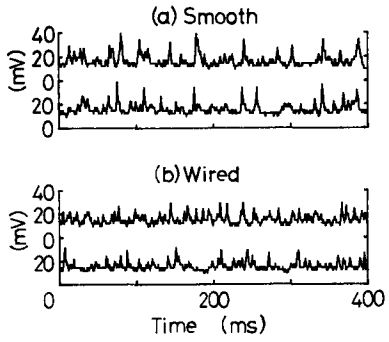

Figure 7. Fluctuation of the liquid film thickness in the (a) smooth column and (b) wired column.

trends are almost the same, although not so clear, as those shown in figure 3 for the inner-wired tube in former studies.

From the measurements in figures 6 and 7 it can be seen that the effect of the centrifugal force on the disturbance waves is not that great, and the direct interaction between the waves and the helical obstacles seems to be the main cause of the smoothing of liquid film surface.

The entrainment may be reduced not only by the decrease in the number of disturbance waves but also by the centrifugal force of the swirling motion of the gas phase. The latter force could explain the decrease in the entrainment in both figures 1 and 6. Köhler & Kastner (1986) and Yoshida *et al.* (1988) have pointed out that the centrifugal acceleration may improve the phase separation and hence the heat transfer in rifled tubes. In the present experiment, however, it was impossible to estimate the effect of the centrifugal force on the phase separation independently from the suppression of droplets by the decrease in the number of disturbance waves. The two effects may act coincidently with each other.

4. CAUSE OF THE DEFORMATION OF DISTURBANCE WAVES

Figure 8 shows the interaction between the disturbance waves and the helical mono-wire obtained at measuring points A–F on the outer surface of the mono-wired column by the electric conductance method. As shown in the figure, point B is located upstream of the wire, where there is no obstacle to the liquid film flow. Hence, the film thickness measured at point B is nearly the same as that of the disturbance waves on the smooth surface. Since points C–F are located downstream of the wire, the liquid supply is restricted and the film thickness becomes thin,

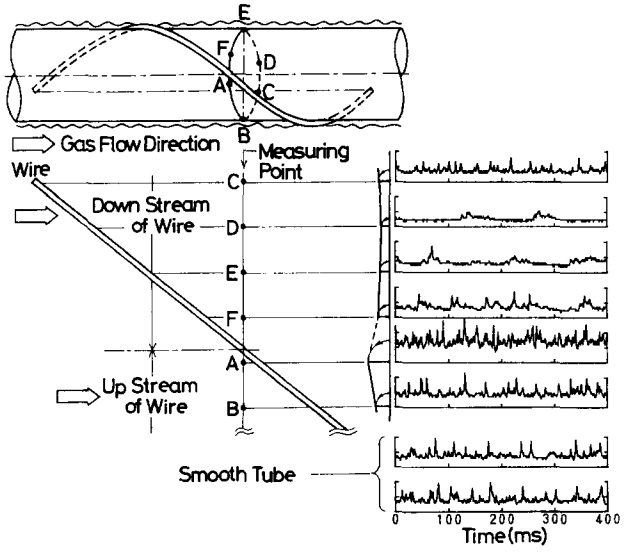

Figure 8. Interaction between the disturbance waves and the helical mono-wire.

especially at points D and E. At the same time, the waves decrease both in number and height, and the film surface becomes smooth.

On the other hand, the result at point A, which is located just upstream of the wire, should be noted. The mean thickness of the film and the wavenumber increase greatly, and the wave becomes small but of a sharp form at point A. Since point A is the location where the liquid film including the disturbance waves collides with the helical wire, it is suggested that a complex flow could be induced in the liquid film at this point—which could influence the form of the surface of the film.

Figure 9 shows the result of a flow visualization obtained by the oil film method. The oil film traces shown in the photograph suggest that direction of the streamline at the middle of a span between two wires is almost parallel with that of the wires. On the other hand, it is found that just upstream of the wires there is a velocity component perpendicular to the previous direction, and the oil film traces make a certain angle with the directions of the wires and the bulk film flow.

The velocity component described above seems to be caused by the fact that the liquid film including the disturbance waves is forced to flow in the helical direction along the wires, whereas it would flow straight along the channel axis with the gas flow in the absence of the wires. The change of flow direction along the wires produces a pressure increase via acceleration in the liquid film at point A, together with an increase in the film thickness. The pressure increase should induce the perpendicular velocity component in the bottom layer of the film flow adjacent to the column surface, since the liquid velocity along the wires is very low in the layer. As a result, the secondary flow should be generated upstream of the wires as shown in figure 9.

These results indicate that large differences in both the velocity and the flow direction, and hence a large velocity gradient, should exist in the film flow at point A. Since the energy of the disturbance waves should be dissipated by a large velocity gradient, it is estimated that the waves change their original shape (as shown in figure 8) and are finally broken into comparatively small waves by the wires, as measured in figures 3 and 7.

The effect of a velocity gradient on sea waves has been investigated theoretically by Sir Geoffrey Taylor (1955) in relation to a breakwater. It also has been confirmed empirically in a deep water tank (Hara *et al.* 1984, 1988) that waves are broken down by a velocity gradient in a surface current proceeding in the inverse direction to that of the waves. The disturbance waves on such a thin liquid

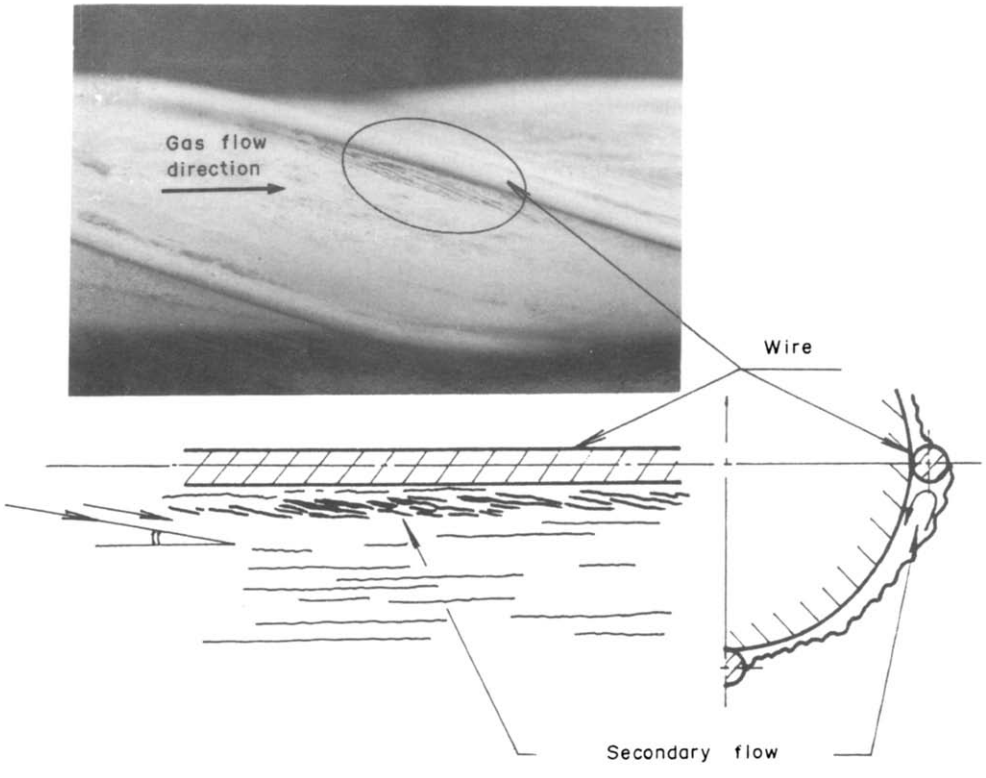

Figure 9. Flow visualization by the oil film traces.

film as that in the present paper should have, of course, different characteristics from waves on deep water. However, since the hydrodynamic force (caused by the velocity gradient) on the fluid particle should be similar, this fundamental feature of the flow with the breakwater could be compared to that in the thin film flow described above.

5. CONCLUSIONS

The effect of helical wires on liquid film structures in annular mist flow was investigated experimentally in a double-tube type channel. The following conclusions were drawn in connection with the cause of the wave deformation in helical-wired channels:

(1) The disturbance waves on the liquid film surface are decreased in number and changed from their original shape by the helical wires on the channel wall as compared with those on a smooth surface. The trend is almost the same as that in an inner-wired tube.
(2) The mean thickness of the liquid film and the wavenumber increase greatly, and the wave becomes small but of a sharp form just upstream of the wire. Furthermore, the secondary flow can be observed in the bottom layer of the liquid film at this point.
(3) It is suggested that the disturbance waves are broken down by the helical obstacles into comparatively small waves, since the energy of the disturbance waves should be dissipated by the large velocity gradient in the liquid film.
(4) The effect of the centrifugal force acting on the disturbance waves is estimated to be small. Therefore, the direct interaction between the waves and the helical obstacles described above seems to be the main cause of the deformation of the disturbance waves, and hence the entrainment suppression.

REFERENCES

HARA, S., IGAI, M. & NAMIE, S. 1984 Fundamental study on air bubble type of oil boom. *Trans. Kansai zosenkyokai* **194,** 1–6 (in Japanese).

HARA, S., IGAI, M. & NAMIE, S. 1988 Development of the air bubble type of oil barrier. In *Preprints of the Techno Ocean Symp.*, Kobe, Vol. 1, pp. 54–59.

IWABUCHI, M., TATEIWA, M. & HANEDA, H. 1982 Heat transfer characteristics of rifled tubes in the near critical pressure region. *Proc. 7th Int. Heat Transfer Conf.* **5,** 313–318.

KÖHLER, W. & KASTNER, W. 1986 Heat transfer and pressure loss in rifled tubes. *Proc. 8th Int. Heat Transfer Conf.* **6,** 2861–2865.

NAMIE, S. & SHIOZAKI, K. 1990 Investigation of annular liquid film flow in tubes with helical ribs and wires (suppression of droplet entrainment with the aim of improving evaporative heat transfer). *Trans. JSME* **56B,** 1113–1118 (in Japanese); 1991 *Heat Transfer Jap. Res.* **20,** 291–305 (in English).

NAMIE, S. & SHIOZAKI, K. 1991 Investigation of annular liquid film flow in tubes with helical ribs and wires (suppression of droplet entrainment with the aim of improving evaporative heat transfer). In *Preprints of the 3rd ASME/JSME Thermal Engineering Joint Conf.*, Reno, NV, Vol. 2, pp. 223–228.

SHIOZAKI, K. & NAMIE, S. 1991 Investigation of annular liquid film flow in tubes with helical ribs and wires (experimental correlation and cause of the entrainment suppression effect). *Trans. JSME* **57B,** 1316–1320 (in Japanese); 1991 *Heat Transfer Jap. Res.* **20,** 782–792 (in English).

TAYLOR, SIR G. I. 1955 The action of a surface current used as a breakwater. *Proc. R. Soc. Lond.* **A231,** 466–478.

YOSHIDA, S., MORI, H., OISHI, K. & OHNO, M. 1988 Improvement of critical heat flux of rifled tubes. In *Preprints of the 25th Natn. Heat Transfer Symp.*, Vol. 1, pp. 295–297 (in Japanese).